International Journal of Mechanical Sciences 52 (2010) 485–494

Contents lists available at ScienceDirect

International Journal of Mechanical Sciences

journal homepage: www.elsevier.com/locate/ijmecsci

The three-point bending of Y-frame and corrugated core sandwich beams

V. Rubino, V.S. Deshpande *, N.A. Fleck

Cambridge University, Engineering Department, Trumpington Street, Cambridge, CB2 1PZ, UK

ARTICLE INFO

Article history:
Received 2 December 2008
Received in revised form
10 November 2009
Accepted 11 November 2009
Available online 29 December 2009

Keywords:
Sandwich beams
Y-frame core
Three-point bending

ABSTRACT

Sandwich beams comprising Y-frame and corrugated cores have been manufactured by assembling and brazing together pre-folded AISI type 304 stainless steel sheets. The longitudinal axis of the cores coincides with the axis of the beams. The quasi-static three-point bending response of both simply supported and clamped beams is measured along with the indentation response of the beams placed on a rigid foundation. The investigation reveals that the initial collapse strength of the beams is governed by the indentation of the Y-frame or corrugated core for all beam geometries considered here. The simply supported beams have a softening response beyond the initial peak load while the clamped beams display a hardening response due to the longitudinal stretching of the face-sheets. The experimental investigation reveals that sandwich beams with Y-frame or corrugated cores have comparable responses for each of the loading situations considered. Additional insight into the deformation modes is obtained by three-dimensional finite element (FE) calculations.

1. Introduction

Over the last decade the design of crashworthy ship structures has focused on double-hull structures, see for example the review by Paik [1] on innovative double-hull designs. There is increasing industrial interest in the replacement of double hulls (and monolithic hulls) by sandwich construction in order to enhance stiffness, strength and energy absorption of ship structures. Recently, a range of topologies of lattice material have been devised for sandwich cores. These materials include the pyramidal truss, the tetrahedral truss and the metal textile core [2,3]. These topologies deform by axial extension of the constituent members with only a minor contribution from the bending stiffness of the struts [4]. Consequently, they have high specific stiffness and strength. On the other hand, bending-governed micro-structures such as metallic foams and an egg-box material based upon a solid sheet or a wire mesh have much lower stiffness and strength than the above lattices materials (for a given relative density). However, the choice of core topology for crash-resistant ship structures remains unclear—it is anticipated that structures that maximize energy absorption without undergoing failure by sheet tearing are optimal for use as crash-resistant structures. One of the objectives of this paper is to analyze two sandwich core topologies that help minimize the tensile strains that develop in the structure when deformed quasi-statically.

There may be structural advantages in the use of weak sandwich cores in a ship hull over strong cores: the weak core is able to diffuse an external transverse load over a larger volume of hull without perforation, and reduce the propensity for shear-off of the sandwich panel from the supporting sub-structure, see for example Naar et al. [8]. A recent example is the high crashworthiness of a Y-shaped sandwich core, manufactured by welding together steel sheets, as proposed by Schelde Shipbuilding[1] (Fig. 1a). Full scale tests have shown that the Y-frame double-hull has a significantly higher resistance to tearing than conventional single skin design [5,6]. The finite element simulations of Konter et al. [7] adequately capture the response of the tested Y-frame structure. A competing concept to the Y-frame core for ship hull construction is the corrugated core (Fig. 1b), known as the Navtruss and developed by Astech.[2] The aim of the current study is to compare these two competing concepts under idealised loadings that broadly mimic a low speed ship collision. It might be anticipated that the Y-frame core is significantly weaker than the corrugated core, as the Y-frame bends rather than stretched under transverse compression. Remarkably, we shall find that the two cores are broadly similar in response, and we subscribe this to the high longitudinal shear strength of both types of core. The details are given below.

The structural response of Y-cores has been explored in a limited number of numerical and experimental studies. Pedersen et al. [9] performed a finite element investigation of the compressive response of the Y-frame. They developed contour

* Corresponding author. fax: +44 1223 332662.
E-mail address: vsd@eng.cam.ac.uk (V.S. Deshpande).

[1] Royal Schelde, P.O. Box 16 4380 AA Vlissingen, The Netherlands.
[2] Astech Engineering Products, 3030 Red Hill Ave, Santa Ana, CA 92705, USA.

0020-7403/$ - see front matter © 2009 Elsevier Ltd. All rights reserved.
doi:10.1016/j.ijmecsci.2009.11.009

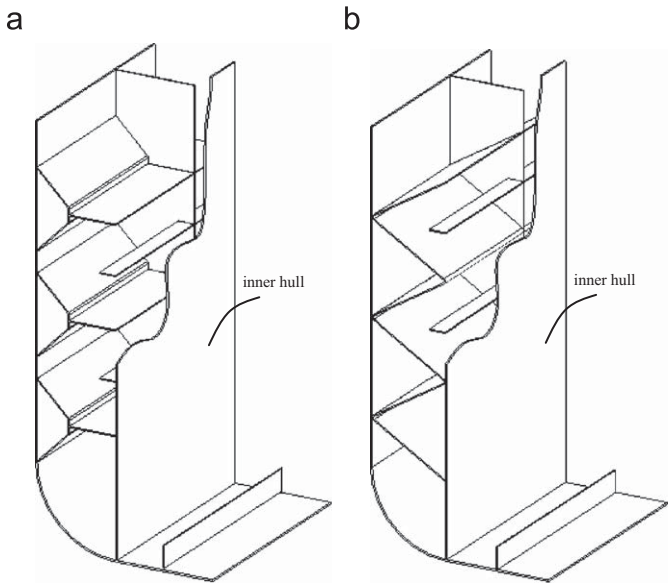

Fig. 1. Sketch of the (a) Y-frame and (b) corrugated sandwich cores as used in ship hull construction. The core is sandwiched between the outer and inner hulls of the ship.

plots of through-thickness compressive strength and energy absorption of the Y-frame with the geometric parameters of the Y-frame as axes of these maps. Subsequently, Rubino et al. [10] investigated the transverse compressive and shear strength of the Y-frame core in a combined experimental and finite element study. They also measured the indentation response of sandwich beams with a Y-frame core and resting upon a rigid foundation concluded that the relatively high indentation strength was due to the high longitudinal shear strength of the core.

The three-point bending behaviour of metallic sandwich beams has been extensively investigated for both the simply supported state and the fully clamped state. For example, the response of simply supported sandwich beams has been determined for a metal foam core [11–13], truss cores [14,15] and a corrugated core [16]. Likewise, the collapse response of clamped beams has been addressed for square-honeycomb cores [17] and metal foam cores [18]. However, no systematic investigation has been reported on the quasi-static bending response of Y-frame core sandwich beams. This is needed in order to gauge the comparative performance of crash-resistant Y-frame hull structures with competing designs.

The main aim of the current study is to develop an understanding for the collapse response of clamped and simply supported sandwich beams with Y-frame cores and contrast their performances with equivalent corrugated sandwich beams. This behaviour is relevant for understanding the slow speed crash response of say ship hulls and vehicle frames made from such structures—while Rubino et al. [10] have thoroughly investigated the response of the Y-frame core under shear, compression and indentation, no investigation to-date has been reported on the bending response of Y-frame (and corrugated) core sandwich beams. This study aims to fill this gap in understanding.

The outline of the paper is as follows. First, the manufacture of laboratory scale Y-frame and corrugated core sandwich beams is described. Next, the three-point bending responses of clamped and simply supported beams are measured, along with the indentation behaviour of these beams placed on a rigid foundation. Finally, the measured responses are compared with three-dimensional finite element calculations.

2. Experimental investigation

Quasi-static three-point bend tests were conducted on clamped and simply supported beams with Y-frame and corrugated cores. The primary objectives of the experimental investigation are as follows:

(i) To compare the quasi-static bending response of the clamped and simply supported beams and to determine the dominant collapse mechanisms.
(ii) To contrast the quasi-static responses of sandwich beams with the corrugated and Y-frame prismatic core topologies.
(iii) To explore the ability of three-dimensional finite element calculations to predict the quasi-static response of the sandwich beams.

2.1. Specimen manufacture

Scaled-down Y-frame cores of two sizes were manufactured from AISI 304 stainless steel. An approximately 1/10 scale Y-frame core was of depth c=44 mm and width b=115 mm was made from sheets of thickness g=0.5 mm. Also, an approximately 1/20 scale core was of depth c=22 mm, width b=52 mm was made from g=0.3 mm thick sheets. Subsequently, these two cores shall be referred "large" and "small" Y-frame cores, respectively. The cross-sectional dimensions of the large and small Y-frame cores are given in Figs. 2a and b, respectively. A global co-ordinate reference frame is included in the figure in order to clarify the various directions: x_1 is the longitudinal axis of the Y-frame, x_2 denotes the transverse direction and x_3 is the out-of-plane direction for the sandwich beam. The Y-frames are close-packed along the x_2-direction such that adjacent Y-frames touch; the relative densities of the as-manufactured large and small Y-frame sandwich cores (that is, the ratio of effective density of the smeared-out core to that of the parent solid material) are $\overline{\rho} = 2.1\%$ and 2.5%, respectively.

Both the large and small Y-frame sandwich cores were manufactured using the same processing route. The stainless steel sheets were computer-numerical-control (CNC) folded to form the upper part of the Y-frame and the Y-frame leg. Slots were then CNC-cut into the Y-frame web and the Y-frame leg was fitted into the upper part of the Y-frame, as described in [10]. The assembly comprising two Y-frames (Figs. 2a and b) was then spot welded to face-sheets and a Ni–Cr 25-P10 (wt%) braze alloy applied uniformly over all sheets of the assembly. The assembly was then brazed together in a vacuum furnace at 1075 °C in a dry argon atmosphere at 0.03–0.1 mbar. Finally, the beams were water-jet cut to the required length.

Corrugated core sandwich beams with a core relative density $\overline{\rho} = 2.5\%$ were also manufactured and tested; they had the same overall dimensions as the sandwich beams with the small Y-frame core. The corrugated core comprised four sheets inclined at 60° (Fig. 2c) and was manufactured by CNC folding 0.3 mm thick 304 stainless steel sheets. This folded section was then brazed to the sandwich beam face-sheets in order to obtain a sandwich beam with two corrugations along the x_2-direction (Fig. 2c) to give a core of width b=55 mm.

2.2. Specimen configurations for the three-point bend tests

Simply supported and end-clamped sandwich beams were tested, with the x_1-axis of the cores aligned parallel to the longitudinal axis of the beams, see Figs. 3a and b and a width b in

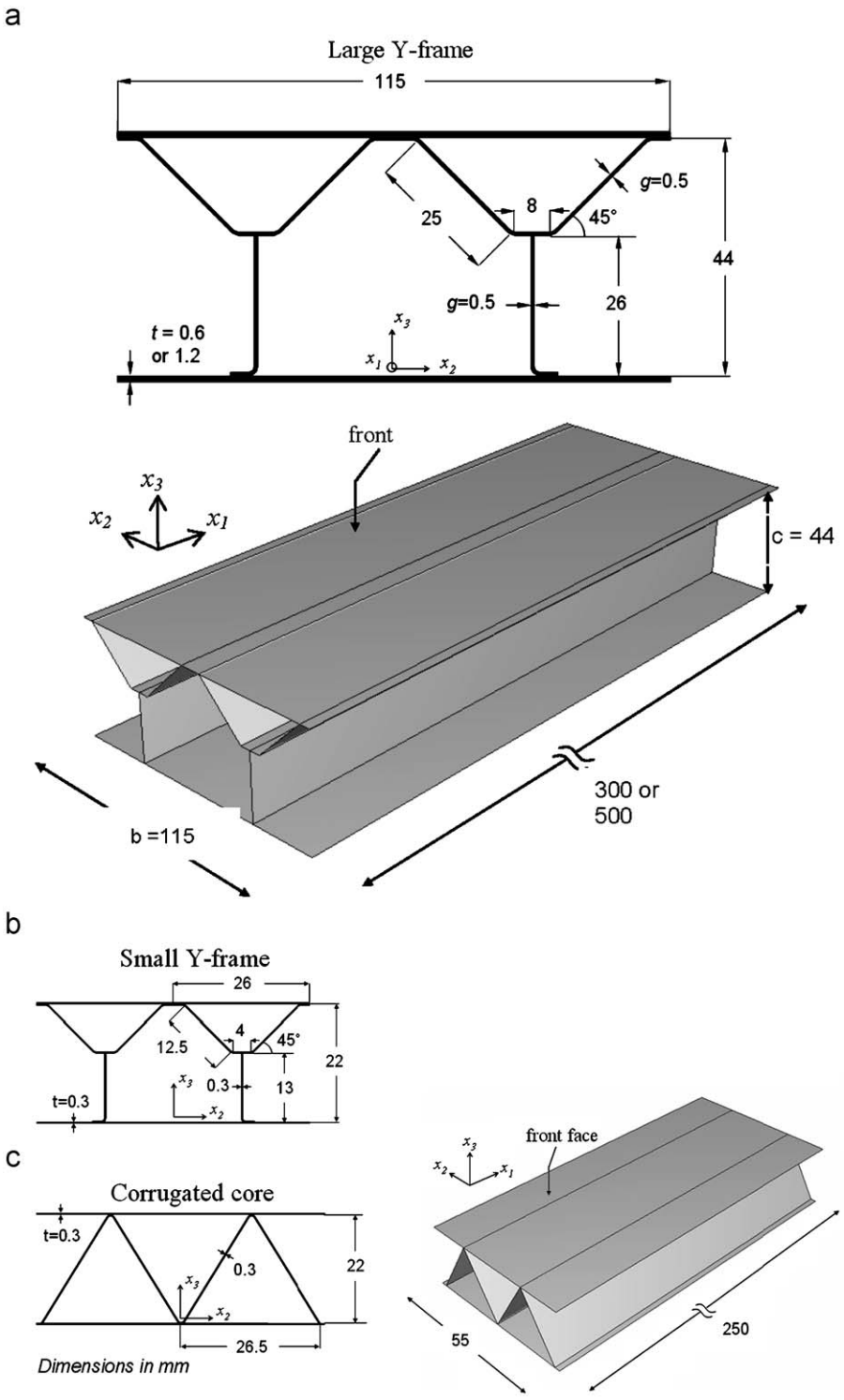

Fig. 2. Geometries of the (a) large Y-frame, (b) small Y-frame and (c) corrugated sandwich cores. All dimensions are in mm and the co-ordinate systems employed are displayed.

the x_2-direction. In order to probe the collapse modes and compare the Y-frame and corrugated core sandwich beams, five geometries of the Y-frame core sandwich beams and one geometry of the corrugated core beam were considered as detailed in Table 1. The bulk of the investigation was carried out on sandwich beams made from the large Y-frame core; these beams were of spans $2L=300$ and 500 mm and comprised face-sheets of thickness $t=0.6$ and 1.2 mm (Table 1). In addition, in order evaluate the effect of core topology on sandwich beam performance we also tested sandwich beams with the small Y-frame core and the corrugated core. These beams had a span $2L=250$ mm and face-sheets of thickness $t=0.3$ mm (geometries 5 and 6 in Table 1). Note that geometries 5 and 6 possess identical overall dimensions and mass, and differ only in terms of core topology.

All geometries of Table 1 were tested in both the simply supported and the end-clamped configurations, as sketched in Figs. 3a and b. In order to achieve a fully clamped boundary

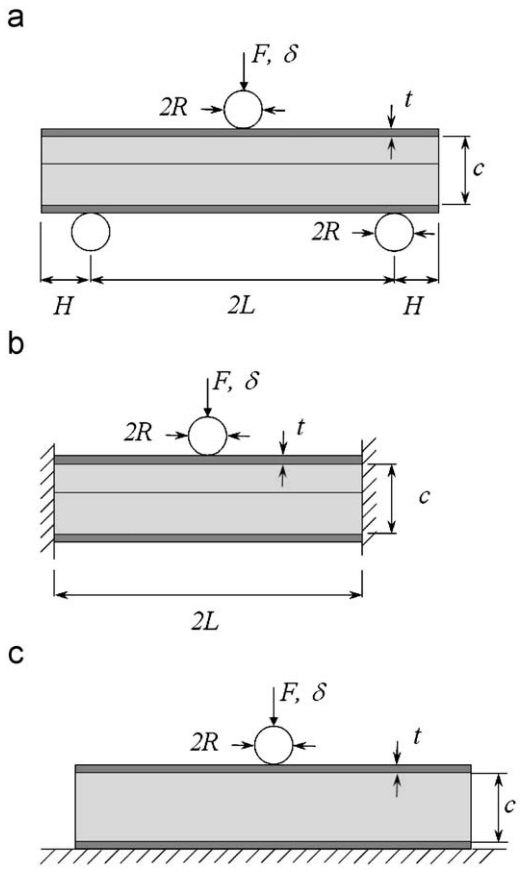

Fig. 3. Sketches of the (a) simply supported and (b) clamped three-point bending arrangements. (c) An illustration of the indentation of the sandwich beams placed on a rigid foundation. The important dimensions of the beams and loading rollers are labelled on the figure.

Table 1
A summary of the sandwich beam geometries employed in this study.

Specimen	Core type	2*L* (mm)	*t* (mm)	*b* (mm)
1	Large Y-frame	300	0.6	115
2	Large Y-frame	300	1.2	115
3	Large Y-frame	500	0.6	115
4	Large Y-frame	500	1.2	115
5	Small Y-frame	250	0.3	52
6	Corrugated	250	0.3	55

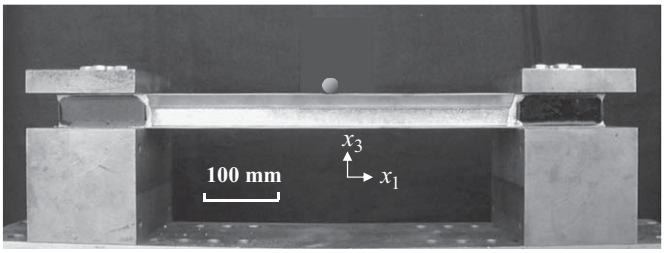

Fig. 4. Photograph of the clamped sandwich beam (t=0.6 and 2L=500 mm) with the large Y-frame core. The end portions of the beam are infiltrated with epoxy and are then clamped.

condition on the beam ends, end portions of the beam were bolted onto the test rig, as shown in the photograph of Fig. 4. The ends of the beam were gripped as follows. The sandwich core at the ends of the beams were filled with an epoxy resin to make the sandwich core fully dense. The end portions of the sandwich beams were then bolted to the test-rig via steel clamping plates and M8 bolts, see Fig. 4.

2.3. Properties of the constituent materials

Tensile specimens of dog-bone geometry were cut from the as-received 304 stainless steel sheets and were subjected to the same brazing cycle as that used to manufacture the sandwich beams. The measured true stress versus logarithmic strain response at a tensile strain rate of $\dot{\varepsilon} = 10^{-3}\,\mathrm{s}^{-1}$ is given in Fig. 5. The stainless steel behaves in an elastic–plastic manner with a Young's modulus E=210 GPa, a yield strength of σ_Y=210 MPa and displays linear hardening in the plastic regime with a tangent modulus of $E_t \approx 2.1$ GPa.

For reference purposes, the quasi-static out-of-plane compressive (σ_{33} versus ε_{33}) and longitudinal shear (σ_{13} versus γ_{13}) responses of the large Y-frame core are shown in Figs. 6a and b, respectively, from Rubino et al. [10]. The compressive response of the Y-frame core has an initial elastic response, a peak stress of about 0.54 MPa and subsequently softens. In contrast, the longitudinal shear response has an initial elastic branch followed by an almost ideally plastic response and a peak shear strength of approximately 1.7 MPa.

3. Experimental results

The three-point bending experiments were carried out on a 100 kN screw driven test machine with the central roller (Fig. 3) displaced at a rate of $\dot{\delta} = 0.005\,\mathrm{mm\,s}^{-1}$. The central roller was located on the front face, as defined in Fig. 2. The applied load F was measured via the load cell of the test machine while the central roller displacement δ was recoded using a laser extensometer. A second laser extensometer was used to measure the relative displacement δ_I between the two face-sheets of the beam at mid-span. Hereafter, we shall refer to the relative displacement δ_I as the 'indentation'.

The measured three-point bending responses of the simply supported and clamped beams are presented in two steps. First, the response of the sandwich beams with the large Y-frame core is reported and then a comparison of the responses is presented

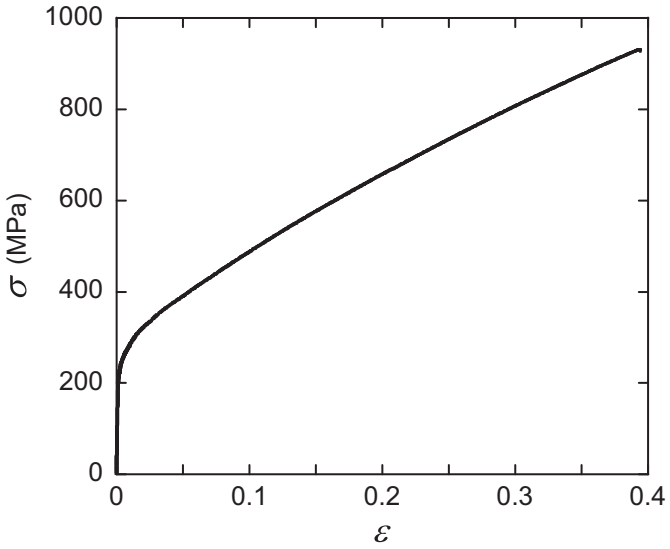

Fig. 5. The quasi-static true tensile stress versus logarithmic strain response of the as-brazed 304 stainless steel used to manufacture the sandwich beams.

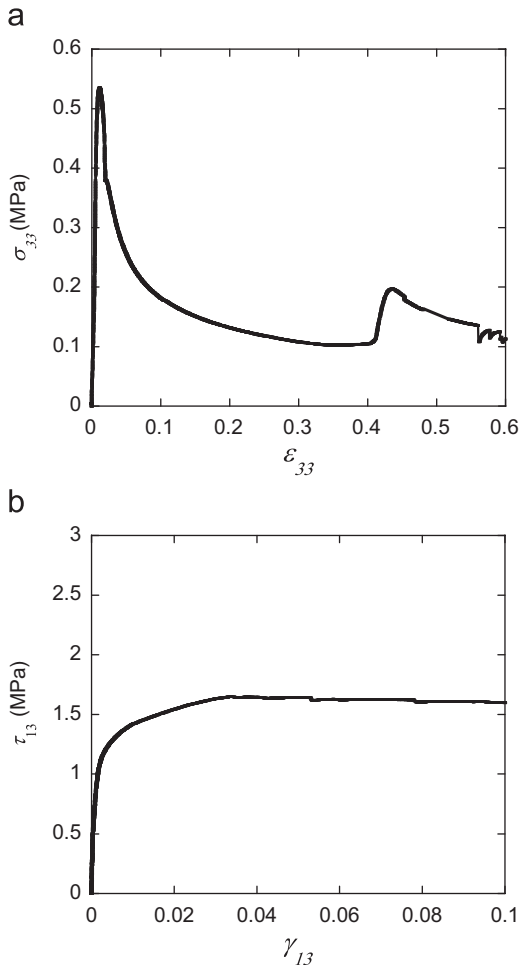

Fig. 6. The measured (a) out-of-plane compressive and (b) longitudinal shear responses of the large Y-frame core. The co-ordinate system employed to label the stresses and strain are marked in Fig. 2. Reproduced from Rubino et al. [10].

for the sandwich beams with the small Y-frame core and with the corrugated core.

3.1. Response of the sandwich beams with the large Y-frame core

The three-point bending response of sandwich beams with the large Y-frame core was measured using cylindrical rollers of radius R=9 mm. The measured normalised load $\overline{F} \equiv F/(\sigma_Y bt)$ versus normalised displacement $\overline{\delta} \equiv \delta/L$ responses of the sandwich beams (face sheet thickness t=1.2 mm) with the large Y-frame core are shown in Figs. 7a and 8a for beams of span $2L$=300 and 500 mm, respectively. In the normalisation of the load, σ_Y=210 MPa is the measured yield strength of the as-brazed 304 stainless steel from which the Y-frame sandwich beams are constructed, b=115 mm is the width of the beams in the x_2-direction and t=1.2 mm is the face sheet thickness. In all cases, the load versus displacement response is characterized by an initial elastic regime followed by an initial peak load F_{peak}. Subsequently, the simply supported beams undergo softening while the clamped beams display a strongly hardening response due to longitudinal stretching of the face-sheets (and core).

The measured normalised initial peak loads $\overline{F}_{peak} \equiv F_{peak}/(\sigma_Y bt)$ are summarized in Table 2. Observe that the initial peak loads F_{peak} are approximately equal for the clamped and simply supported beams and reasonably independent of the span L. These observations suggest that the peak load of the beams is

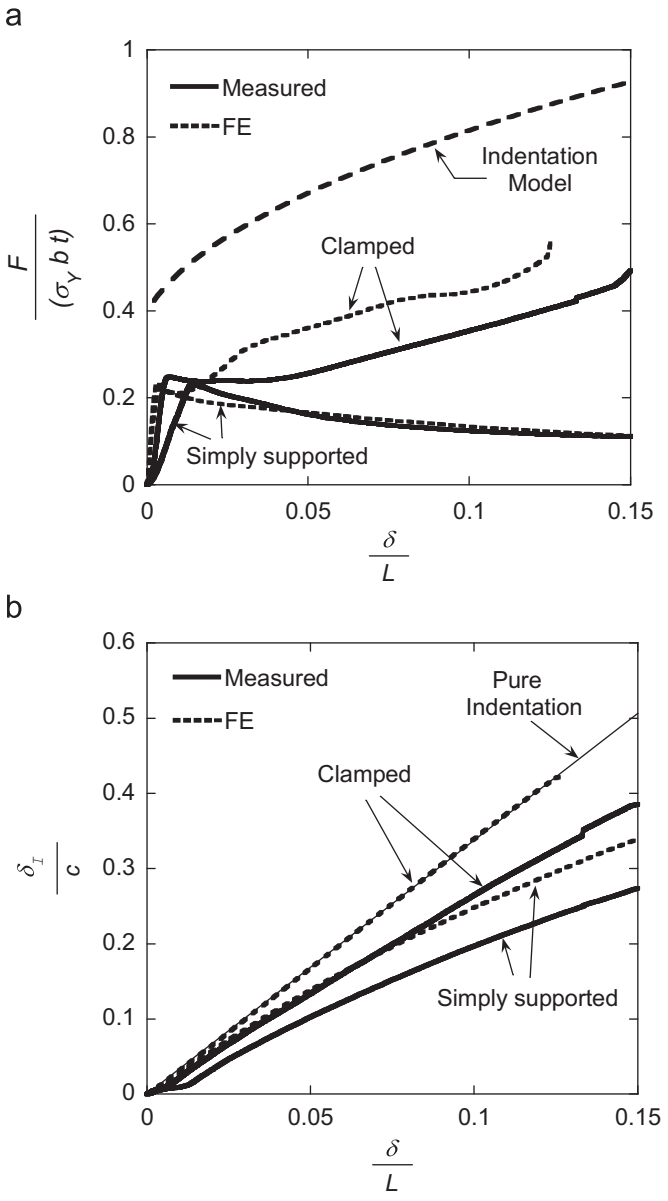

Fig. 7. The measured three-point bending responses of simply supported and end-clamped sandwich beams (span $2L$=300 mm and face sheet thickness t=1.2 mm) with the large Y-frame core. (a) The normalised applied force F versus central roller displacement δ and (b) the normalised indentation displacement δ_I versus central roller displacement δ. In (b) the line corresponding to pure indentation δ_I=δ is included. The FE predictions of the responses are plotted in (a) and (b), and the predictions of the analytical indentation model are included in (a).

dominated by indentation of the core rather than bending of the beams. We test this hypothesis by comparing the indentation displacement δ_I with the total displacement δ at the peak load, as follows.

The indentation displacement δ_I versus δ characteristics are plotted in Figs. 7b and 8b for the beams with spans $2L$=300 and 500 mm, respectively. For comparison purposes, the figures include the line corresponding to pure indentation absent any bending, that is δ=δ_I. At $\delta/L \approx 0.01$, peak load is attained in the three-point bending tests and at this stage of deformation the indentation displacements are significantly larger than the bending deflections δ–δ_I. This suggests that peak load is dominated by the indentation of the Y-frame core. To further support this, consider the indentation of Y-frame beams on a rigid

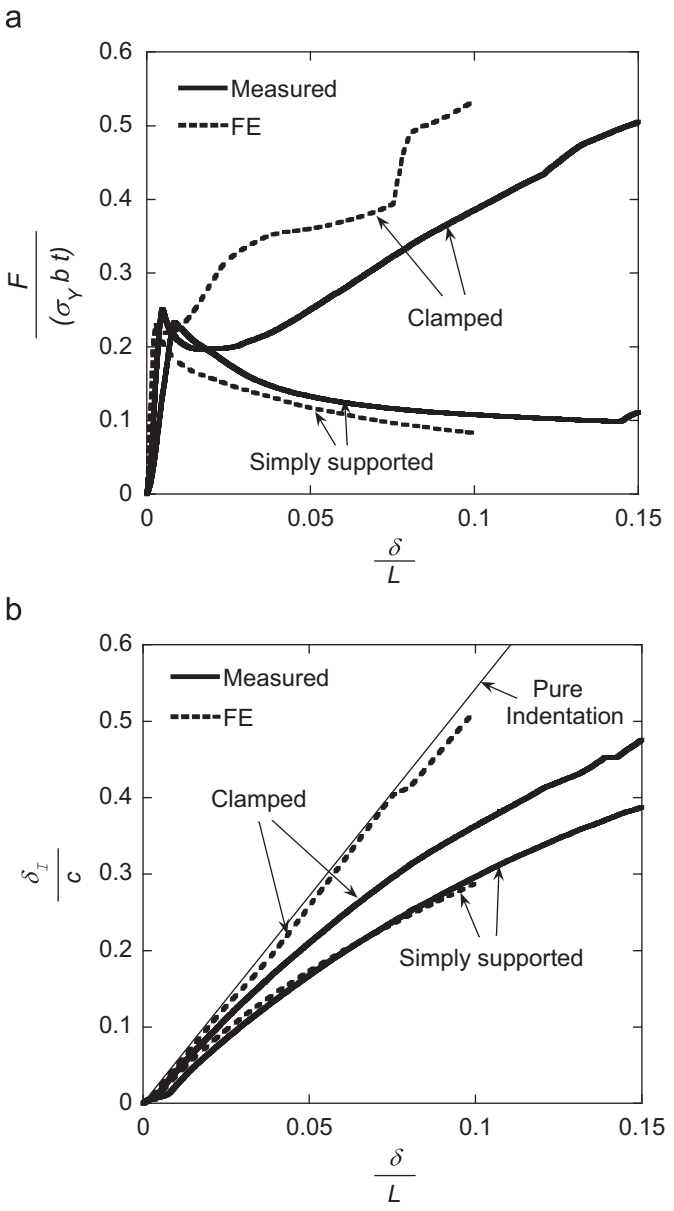

Fig. 8. The measured three-point bending responses of simply supported and clamped sandwich beams (span $2L$=500 mm and face sheet thickness t=1.2 mm) with the large Y-frame core. (a) The normalised applied force F versus central roller displacement δ and (b) the normalised indentation displacement δ_I versus central roller displacement δ. In (b) the line corresponding to pure indentation $\delta_I=\delta$ is included. The FE predictions of the responses are plotted in (a) and (b).

foundation (Fig. 3c). Such indentation measurements with R=9 mm cylindrical indenters were performed by Rubino et al. [10] on Y-frame sandwich beams of length 600 mm but otherwise identical to those considered here. The normalised initial peak indentation loads from those measurements for sandwich beams with t=12 and 0.6 mm thick face-sheets are included in Table 2: these peak indentation loads are approximately equal to those measured in the three-point bend tests on the clamped and simply supported beams.

We conclude that the initial peak load of the Y-frame beams under three-point bending is governed by core indentation. An analytical upper bound model for the indentation response of the sandwich beams is presented in Appendix A. Predictions of this model are included in Fig. 7a. While the model captures the hardening rate of the clamped beams, it significantly over-predicts the loads.

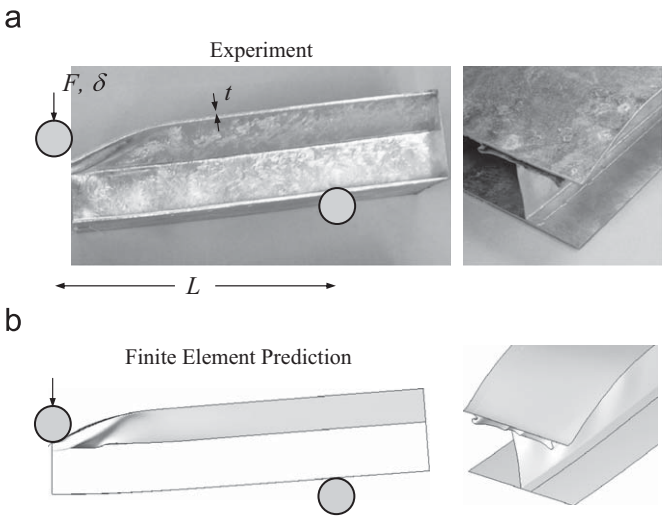

Fig. 9. The (a) observed and (b) FE predictions of the deformation mode of the simply supported sandwich beam ($2L$=300 and t=1.2 mm) with the large Y-frame core. The images are for beams loaded to $\delta \approx 25$ mm and then unloaded. A side view along the x_2-direction showing half the beam and a view of the deformation of the core obtained by sectioning the beam along the mid-span are included.

Photographs of the deformed $2L$=300 mm simply supported and clamped sandwich beams with t=1.2 mm face-sheets are included in Figs. 9a and 10a, respectively. These photographs were taken after deforming the beams to $\delta \approx 25$ mm and then unloading. Two views are shown in the figures: (i) a side view along the x_2-direction showing half the beam and (ii) a view of the deformation of the core obtained by sectioning the beam at mid-span. The photographs confirm that indentation of the core is the main contributor to the displacement δ of the central roller, with the rear face sheet undergoing negligible displacement. Hence, the initial peak load is approximately equal for both the simply supported and clamped beams.

The responses of the simply supported and clamped beams at large deflections are markedly different. While the simply supported beams display a softening response, longitudinal stretching of the face-sheets (and core) endows the clamped beams with a hardening response. In order to quantify these differences we define an average force F_{avg} over a range δ_c of roller displacements as

$$F_{avg} \equiv \frac{1}{\delta_c}\int_0^{\delta_c} F\,d\delta. \tag{1}$$

The normalised average loads $\overline{F}_{avg} \equiv F_{avg}/(\sigma_Y bt)$ are reported in Table 2 for δ_c=8.8 mm. Clearly $\overline{F}_{avg}$ is higher for the clamped beams than the simply supported beams. It is also noted that $\overline{F}_{avg}$ is approximately equal for the clamped beams of span $2L$=300 mm and for the beams on a rigid foundation. To rationalise this, recall that even at large values of δ, the $2L$=300 mm clamped beam is sufficiently stiff in bending that the primary deformation mode is core indentation (Fig. 10a) and thus $\overline{F}_{avg}$ is equal for both these tests. However, $\overline{F}_{avg}$ is lower for the $2L$=500 mm clamped beam as significant bending does occur in these beams at high values of δ.

3.2. Comparison of the responses of the Y-frame and corrugated core beams

Experimental and FE investigations by Rubino et al. [10] and Cote et al. [19] indicate that Y-frame and corrugated cores of the same relative density $\overline{\rho}$ have comparable strengths in transverse compression, and also have comparable strengths in longitudinal

Table 2
A summary of the measurements, FE and analytical predictions of the peak load F_{peak} and average load F_{avg} for the three-point bending of the sandwich beams with the large Y-frame cores. The corresponding measurements and predictions of F_{peak} and F_{avg} for the indentation of sandwich beams with the large Y-frame cores placed on a rigid foundation are also included from Rubino et al. [10].

Specimen			Non-dimensional peak load, $F_{peak}/\sigma_Y bt$			Non-dimensional average load, $F_{avg}/\sigma_Y bt$	
Boundary Condition	Specimen geometry		Measured	FE	Analytical	Measured	FE
	Span (mm)	Face sheet thickness (mm)					
Simply Supported	300	0.6	0.43	0.32	0.69	0.29	0.21
		1.2	0.25	0.23	0.39	0.16	0.14
	500	0.6	0.39	0.28	0.69	0.24	0.14
		1.2	0.23	0.21	0.39	0.16	0.12
Clamped	300	0.6	0.42	0.34	0.69	0.38	0.44
		1.2	0.25	0.24	0.39	0.22	0.27
	500	0.6	0.37	0.30	0.69	0.29	0.35
		1.2	0.25	0.23	0.39	0.18	0.22
Indentation on rigid foundation		0.6	0.40	0.31	0.69	0.38	0.39
		1.2	0.27	0.23	0.39	0.23	0.24

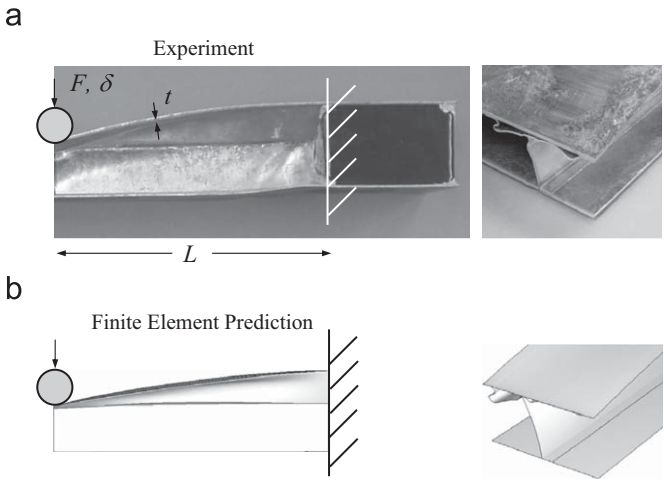

Fig. 10. The (a) observed and (b) FE predictions of the deformation mode of the clamped sandwich beam ($2L$=300 and t=1.2 mm) with the large Y-frame core. The images are for beams loaded to δ=25 mm and then unloaded. A side view along the x_2-direction showing half the beam and a view of the deformation of the core obtained by sectioning the beam along the mid-span are included.

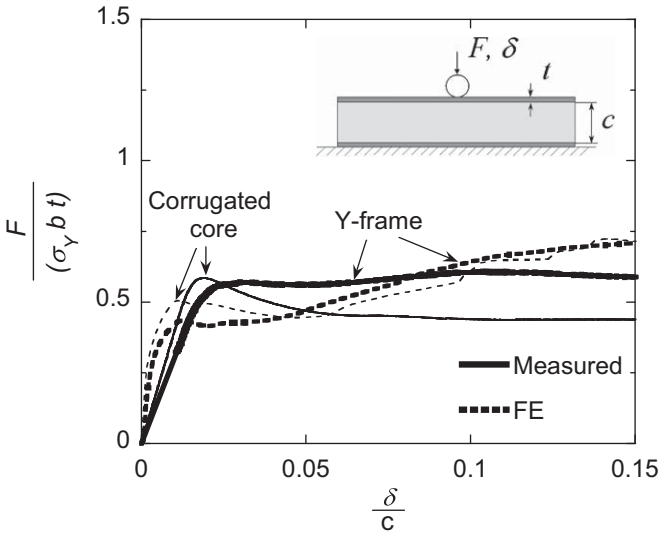

Fig. 11. The measured and FE predictions of the indentation load F versus roller displacement δ response of the sandwich beams placed on a rigid foundation. Measurements for sandwich beams with small Y-frame and corrugated cores corresponding to geometries 5 and 6 in Table 1 are included.

shear. This suggests that Y-frame and corrugated core beams should have similar responses in three-point bending. We investigate this hypothesis by comparing the measured bending and indentation responses of the Y-frame and corrugated core beams with geometries labelled 5 and 6 in Table 1. These beams are identical in every respect other than core topology.

The measured applied normalised load F versus normalised roller displacement δ response of the sandwich beams (geometries 5 and 6 in Table 1) on a rigid foundation is presented in Fig. 11. The indentation load was applied via a central cylindrical roller of radius R=4.5 mm. In line with the fact that the Y-frame and corrugated cores have similar compressive and shear responses, the indentation responses of the corrugated and Y-frame beams are very similar.

The measured three-point bending force F versus central roller displacement δ responses of simply supported and clamped sandwich beams are presented in Figs. 12a and b, respectively. These measurements were conducted using cylindrical loading rollers of radius R=4.5 mm. Consistent with the results presented above in Section 3.1 and the study by Valdevit et al. [16] on corrugated core sandwich beams, core indentation dominated the initial collapse response of all sandwich beams. This is confirmed by visual observations and by the fact that the initial peak loads for the beam bending tests in Fig. 12 are approximately equal to the measured indentation loads (Fig. 11). Similar to the sandwich beams with the large Y-frame core, the simply supported beams have a softening response beyond the initial peak load while the clamped beams display hardening due to the longitudinal stretching of the face-sheets. The Y-frame beams are stronger than the corrugated core beams with the difference between the two sets of beams more pronounced in the simply supported case. This is contrary to expectations and will be discussed further in the context of the finite element simulations presented in Section 4.

3.3. Discussion on the observed deformation mechanisms

Numerous studies on the quasi-static performance of metallic sandwich beams have outlined the key deformation/failure

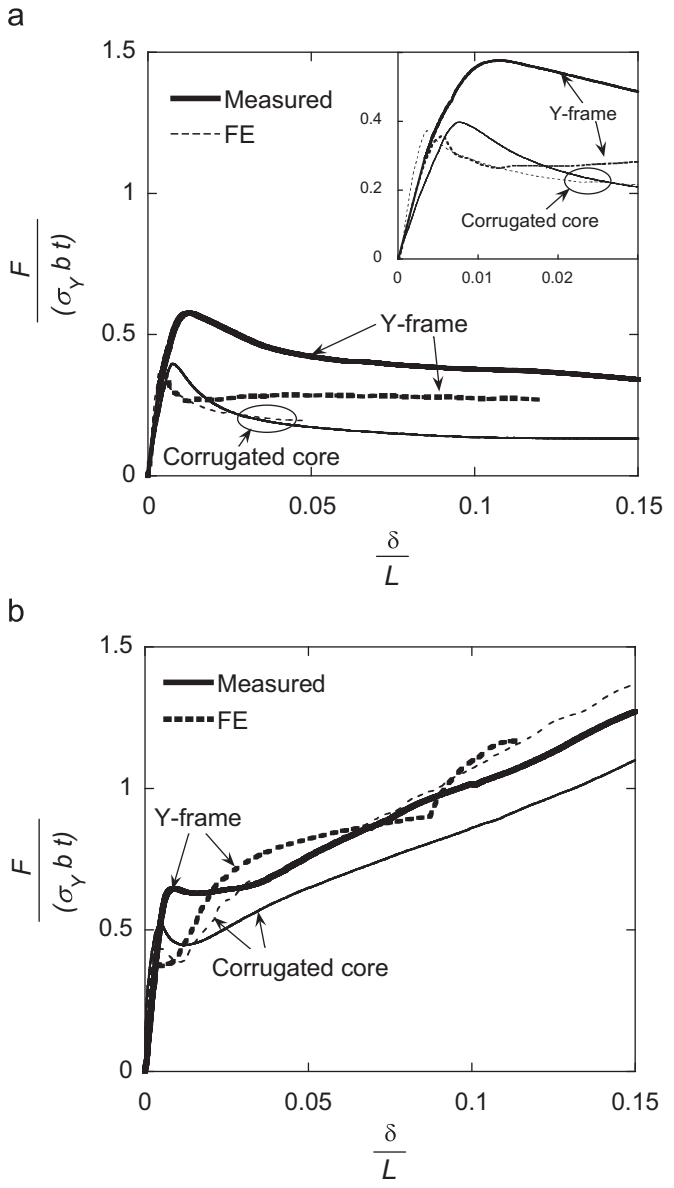

Fig. 12. The three-point bending response of the sandwich beams with the small Y-frame and corrugated cores (geometries 5 and 6 in Table 1). The measured and FE predictions of the applied load F versus roller displacement δ response of the (a) simply supported and (b) clamped sandwich beams.

modes; see for example Ashby et al. [11]. These modes are: (i) core shear, (ii) face yield and (iii) core indentation. Core shear and face yield are often the dominant failure modes in sandwich beams made from cores that have a low shear strength (e.g. metal foams) or sandwich beams with rather thin face-sheets. However, the experimental results discussed above clearly demonstrate that the initial peak load of both the Y-frame and corrugated core beams is set by core indentation. This is due to the fact that both these cores have a rather low compressive strength compared to their longitudinal shear strength (see Fig. 6). In fact their compressive strength is low enough that even face yield will not be operative for most practical sandwich beam designs. It is worth emphasizing here that the low compressive strengths of these cores results in deformation being spread over a large area (see Eq. (A.4) and Appendix A). Thus, these sandwich beams spread the load and reduce strain concentrations near the point of load application- this property is expected to reduce the propensity for sheet tearing and improve the crash resistance of such structures.

4. Finite element simulations

Comparisons of the finite element (FE) predictions and the measured responses of the sandwich beams are presented in this section. All computations were performed in a quasi-static finite deformation setting using the implicit version of the commercially available finite element code ABAQUS[3] (version 6.4).

4.1. Model description

Three-dimensional finite element (FE) simulations of the three-point bending and indentation response of the sandwich beams were conducted. The geometries of the sandwich beams were chosen to match those of the tested specimens (Table 1), with the core cross-sectional dimensions as detailed in Fig. 2.

The face-sheets and core were discretised using 4-noded linear shell elements (S4R in the ABAQUS notation) with a mesh size of 1 mm. The FE model comprised about 60,000 shell elements; a convergence analysis revealed that further refinement of the mesh did not improve the accuracy of the simulations. The hard frictionless contact option was employed in ABAQUS to model contact between the various surfaces in the sandwich beam (e.g. face-sheets and the core). One quarter of the beam was modelled, with symmetry boundary conditions imposed along the mid-span of the beam and along the mid-plane $x_2=0$ (Fig. 2), so that only a single Y-frame or corrugation was modelled in the core. A rigid cylindrical indenter was used to load the beams by imposing an increasing displacement on the roller. Contact between the outer surface of the top face sheet and the rigid indenter was modelled using the frictionless contact option as provided by ABAQUS. In addition, the following boundary conditions were imposed to model the three loading employed in the experiments:

(i) *Simply supported beams*: The quarter beam was rested on a rigid cylindrical roller. Contact between the roller and the outer surface of the bottom face sheet modelled using the frictionless contact option in ABAQUS.
(ii) *Clamped beams*: All translational and rotational degrees of freedom of the beam were constrained on the plane $x_1=L$ to model the clamped boundary conditions.
(iii) *Indentation of beams on a rigid foundation*: All degrees of freedom (rotational and translational) of all nodes on the bottom face-sheet were constrained in order to simulate sticking friction between the rigid foundation and the bottom face-sheet of the sandwich beams.

The stainless steel from which the sandwich beams were constructed was modelled as a rate-independent J2-flow theory solid, with Young's modulus $E=210$ GPa, Poisson ratio $\nu=0.3$ and yield strength $\sigma_Y=210$ MPa. The strain hardening characteristic was tabulated in ABAQUS using data from the measured tensile stress versus strain curve (Fig. 5).

4.2. Comparison of measurements and FE predictions

The FE predictions of the three-point bending response of the simply supported and clamped sandwich beams ($t=1.2$ mm) with the large Y-frame core are included in Figs. 7 and 8 for beams of

[3] Hibbit, Karlsson and Sorensen Inc.

span $2L$=300 and 500 mm, respectively. Overall, there is satisfactory agreement between the measurements and predictions of both the applied load F and the indentation displacement δ_I. The main discrepancies are:

(i) the FE calculations over-predict the hardening of the clamped beams and
(ii) contrary to the measurements, the calculations predict pure indentation of the clamped beams with nearly no deflection of the rear face.

These two discrepancies for the clamped beams are associated with the fact that while perfect clamping was assumed in the FE calculations, the clamped boundary conditions in the experiments permitted some displacement and rotation. The observed hardening response of the beams was thereby reduced and the rear face deflections were increased.

FE predictions of the deformed profiles of the simply supported and clamped Y-frame beams are included in Figs. 9b and 10b, respectively, and allow for direct comparison with photographs of the as-tested specimens. Good agreement between the predicted and observed deformation is obtained in terms of both the side views of the sandwich beams and the deformation of the Y-frame core at mid-span.

A detailed comparison of the predicted and measured peak load F_{peak} and average loads F_{avg} is given in Table 2. While the predicted loads (peak and average) of the beams with face sheet thickness t=1.2 mm are within 10% of the measurements, the predictions for the specimens with t=0.6 mm are less accurate and always under-predict the measurements. We attribute this to the fact that the braze alloy applied over all the sheets of the sandwich beams is not accounted for in the FE calculations; this omission has a greater effect for the sandwich beams with the thinner face-sheets (t=0.6 mm). For the sake of completeness, FE predictions of the peak and average indentation loads for the sandwich beams (with the large Y-frame core) on a rigid foundation are taken from Rubino et al. [10] and included in Table 2. Consistent with the bending FE simulations presented here we observe that the FE predictions of the indentation loads are below the measurements for the sandwich beams with the t=0.6 mm face-sheets.

Comparisons between the FE predictions and measurements of the three-point bending response of the sandwich beams with the small Y-frame core and corrugated core are presented in Fig. 12 while the measured and predicted indentation responses of these beams are included in Fig. 11. The FE predictions again capture the measurements to reasonable accuracy except for the case of the simply supported Y-frame beam (Fig. 12a) wherein the FE calculations substantially under-predict the measurements. While the reason for this discrepancy is unclear it is most likely associated with the fact that excessive braze applied on the tested specimen enhanced the strength of the specimen; this effect was not accounted for in the FE calculations and may explain why the measured response of the Y-frame beams is stronger than the corresponding corrugated core beams.

5. Concluding remarks

Sandwich beams comprising Y-frame and corrugated cores were manufactured by assembling and brazing together pre-folded AISI type 304 stainless steel sheets. The designs of the beams were chosen to represent 1/10 and 1/20 scale versions of the designs used in ship construction by Schelde Shipbuilding. The quasi-static three-point bending response of the beams was measured with the longitudinal axis of the cores aligned with the longitudinal axis of the beams. The initial peak strengths of both the clamped and simply supported beams were approximately equal for the range of beam spans and face sheet thicknesses investigated here. Moreover, these peak strengths were equal to the measured peak indentation strengths of the beams placed on a rigid foundation. This suggests that the initial collapse strength of the beams is governed by indentation of the Y-frame or corrugated core for all beam geometries considered here. The simply supported beams have a softening response beyond the initial peak load while the clamped beams display a hardening response due to the longitudinal stretching of the face-sheets. The measured responses of the beams are also compared with three-dimensional finite element (FE) calculations. These comparisons reveal that the FE calculations capture the measured responses with adequate fidelity.

The experimental investigation revealed that sandwich beams with Y-frame or corrugated cores have comparable responses under all the loading situations considered here (clamped and simply supported three-point bending as well as indentation). Thus, from a purely strength standpoint the Y-frame and corrugated cores have equivalent quasi-static performances.

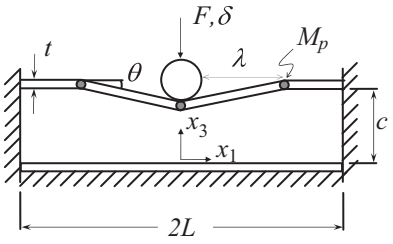

Fig. A1. The assumed deformation mode for the indentation of the Y-frame sandwich beam. The Y-frame sandwich is indented by a cylindrical roller and rests on a rigid foundation.

Acknowledgements

This work was supported by the Netherlands Institute for Metal Research, project No. MC1.03163, The Optimal Design of Y-core sandwich structures.

Appendix A. Analytical model for the indentation response of the sandwich beams

Ashby et al. [11] have introduced an analytical model for the indentation of sandwich beams with a metal foam core. The indentation load was given by additive contributions from compression of the core and from bending of the face-sheets, whereas the contribution due to the shear strength of the foam was neglected. However, the longitudinal shear strength of the Y-frame core significantly exceeds its compressive strength (Fig. 6) and hence Rubino et al. [10] modified the approach of Ashby et al. [11] to include the contribution of the Y-frame core shear strength. The analysis provided an upper bound on the indentation load; comparisons with measurements and with FE predictions in Rubino et al. [10] confirmed the importance of the shear strength of the core.

It is clear from the experiments reported in the current study that the three-point bending response of the clamped sandwich beams entails indentation of the core and stretching of the front face sheet (Fig. 10). The stretching of the front face sheet was not accounted for in the analysis of Rubino et al. [10] and here we modify that analysis so as to apply it to the three-point bending of clamped Y-frame sandwich beams.

The assumed mode of deformation for indentation by a cylindrical roller is sketched in Fig. A1. The Y-frame core and face-sheets are idealised as homogenous rigid, ideally plastic solids. The face-sheets are assumed to have a tensile strength σ_Y while the Y-frame has an out-of-plane compressive strength σ_c in the x_3-direction and a longitudinal shear strength τ_c. Moreover, we assume that the Y-frame can compress in the x_3-direction without straining along the x_1-direction, and that the shear and compressive strengths of the Y-frame are decoupled. Consider the collapse mode as sketched in Fig. A1. The deformation field is written as

$$u(x_1, x_3) = 0 \tag{A.1a}$$

$$v(x_1, x_3) = \begin{cases} \dfrac{\dot\theta}{c}(\lambda - x_1)x_3 & 0 \le x_1 \le \lambda \\ \dfrac{\dot\theta}{c}(\lambda + x_1)x_3 & -\lambda \le x_1 \le 0 \end{cases} \tag{A.1b}$$

where, u and v are material point velocities in the x_1 and x_3 directions, respectively, c is the core thickness and λ is the length of the small segments of the top face sheet that have a rotation rate $\dot\theta$ giving the roller a displacement rate $\dot\delta = \lambda\dot\theta$. The collapse load F (per unit depth in the x_2-direction) can be derived by a simple upper bound calculation as

$$F\lambda\,\dot\theta = 2\sigma_Y t\lambda\dot\varepsilon_f + 4M_P\dot\theta + \sigma_c\int_A \dot\varepsilon_{33}dA + \tau_c\int_A \dot\gamma_{13}dA, \tag{A.2}$$

where the usual strain rate components are $\dot\varepsilon_{33} = \partial v/\partial x_3$ and $\dot\gamma_{13} = \partial v/\partial x_1 + \partial u/\partial x_3$ while the strain rate in the top face sheet $\dot\varepsilon_f$ is estimated as $\dot\varepsilon_f \approx \delta\dot\delta/\lambda^2$. The integrals in (A.2) are over the rectangular region $-\lambda \le x_1 \le +\lambda$ and $0 \le x_3 \le c$ while the plastic bending moment of the face sheet of thickness t is given by $M_P \equiv \sigma_Y t^2/4$. The indentation force reduces to

$$F = 2\frac{t\sigma_Y\delta}{\lambda} + \frac{\sigma_Y t^2}{\lambda} + \sigma_c\lambda + \tau_c c \tag{A.3}$$

The value of the parameter λ is obtained by minimizing F in (A.3) with respect to λ giving

$$\lambda = \sqrt{\frac{2t\sigma_Y}{\sigma_c}\left(\delta + \frac{t}{2}\right)}. \tag{A.4}$$

The two plastic hinges at a distance λ from mid-span travel towards the supports located at $x_1 = L$ (Fig. A1). This provides an upper bound on λ, i.e. $\lambda \le L$. Substituting for λ from (A.4) into (A.3) we get the indentation load versus roller displacement relation as

$$F = \begin{cases} 2\sqrt{t\sigma_Y\sigma_c(2\delta + t)} + \tau_c c & \lambda < L \\ \left(\dfrac{2t\sigma_Y}{L}\right)\delta + \left(\dfrac{\sigma_Y t^2}{L} + \sigma_c L + \tau_c c\right) & \text{otherwise} \end{cases} \tag{A.5}$$

In order to compare the prediction (A.5) with the measured three-point bending response of the clamped sandwich beams with the large Y-frame core we assume the material properties σ_Y=210 MPa (Fig. 5), σ_c=0.5 MPa and τ_c=1.7 MPa (Fig. 6). The comparison between the measurements and analytical predictions is presented in Fig. 7a for the clamped sandwich beam ($2L$=300 and t=1.2 mm) with the large Y-frame core. The model significantly over-predicts the strength of the clamped beams as it does not account for the reduction in the shear strength of the core due to combined compression and shear loading. However, the model captures the hardening rate of the beams with sufficient accuracy suggesting that the stretching effect included here is accurately modelled.

References

[1] Paik JK. Innovative structural designs of tankers against ship collisions and grounding: a recent state-of-the-art review. Mar Technol 2003;40:25–33.
[2] Evans AG, Hutchinson JW, Fleck NA, Ashby MF, Wadley HNG. The topological design of multifunctional cellular metals. Prog Mater Sci 2001;46:309–27.
[3] Wadley HNG, Fleck NA, Evans AG. Fabrication and structural performance of periodic cellular metal sandwich structures. Comput Sci Technol 2003;63:2331–43.
[4] Deshpande VS, Fleck NA, Ashby MF. Effective properties of an octet truss lattice material. J Mech Phys Solids 2001;49:1747–69.
[5] Wevers LJ, Vredeveldt AW. Full scale ship collision experiments 1998. TNO-report 98-CMC-R1725, The Netherlands; 1999.
[6] Ludolphy H. The unsinkable ship—development of the Y-shape support web. In: Proceedings of the second international conference on collision and grounding of ships, Copenhagen, Denmark; 2001.
[7] Konter A., Broekhuijsen J., Vredeveldt A. A quantitative assessment of the factors contributing to the accuracy of ship collision predictions with the finite element method. In: Proceedings of the international conference of ship collisions and grounding, Tokyo, Japan; 2004.
[8] Naar H, Kujala P, Simonsen BC, Ludolphy H. Comparison of the crashworthiness of various bottom and side structures. Mar Struct 2002;15:443–60.
[9] Pedersen CBW, Deshpande VS, Fleck NA. Compressive response of the Y-shaped sandwich core. Eur J Mech—A/Solids 2006;25:125–41.
[10] Rubino V, Deshpande VS, Fleck NA. The collapse response of sandwich beams with a Y-frame core subjected to distributed and local loading. Int J Mech Sci 2008;50:233–46.
[11] Ashby M, Evans A, Fleck N, Gibson L, Wadley H. In: Metal foams: a design guide. Oxford: Butterworth Heinemann; 2000.
[12] McCormack TM, Miller R, Kesler O, Gibson LJ. Failure of sandwich beams with metallic foam cores. Int J Solids Struct 2001;38:4901–20.
[13] Bart-Smith H, Hutchinson JW, Evans AG. Measurement and analysis of the structural performance of cellular metal sandwich construction. Int J Mech Sci 2000;43:1945–63.
[14] Deshpande VS, Fleck NA. Collapse of truss core sandwich beams in 3-point bending. Int J Solids Struct 2001;38:6275–305.
[15] Rathbun HJ, Wei Z, He MY, Zok FW, Evans AG, Sypeck DJ, et al. Measurement and simulation of the performance of a lightweight metallic sandwich structure with a tetrahedral truss core. J Appl Mech 2004;71:368–74.
[16] Valdevit L, Wei Z, Mercer C, Zok FW, Evans AG. Structural performance of near-optimal sandwich panels with corrugated cores. Int J Solids Struct. 2006;43:4888–905.
[17] Zok FW, Rathbun H, He M, Ferri E, Mercer C, McMeeking RM, et al. Structural performance of metallic sandwich panels with square honeycomb cores. Philos Mag 2005;85:3207–34.
[18] Tagarielli VL, Fleck NA. A comparison of the structural response of clamped and simply supported sandwich beams with aluminium faces and a metal foam core. J Appl Mech 2005;72:408–17.
[19] Côté F, Deshpande VS, Fleck NA, Evans AG. The compressive and shear responses of corrugated and diamond lattice materials. Int J Solids Struct 2006;43:6220–42.